2006

Liquid-Flooded Ericsson Cycle Cooler: Part 2 – Experimental Results

Jason Hugenroth
Purdue University

James Braun
Purdue University

Eckhard Groll
Purdue University

Galen King
Purdue University

LIQUID-FLOODED ERICSSON CYCLE COOLER: PART 2- EXPERIMENTAL RESULTS

Jason HUGENROTH[1,*], Jim BRAUN[2], Eckhard GROLL[3], Galen KING[4]

Purdue University, Mechanical Engineering, Herrick Laboratories
West Lafayette, Indiana, USA
[1]jhugenro@purdue.edu
[2]jbraun@purdue.edu
[3]groll@purdue.edu
[4]kinggb@purdue.edu

[*]Corresponding author

ABSTRACT

An experimental test program was conducted on a novel Ericsson cycle heat pump. The concept uses liquid flooding of the compressor and expander to approach isothermal compression and expansion processes. Open drive automotive scrolls were used in the experimental system. Numerous experiments were run at various conditions using nitrogen as the refrigerant and alkyl-benzene oil as the flooding liquid. Volumetric cooling capacities of over 110 kJ/m^3 were measured, and second law efficiencies of approximately 3% were achieved. Similar to other gas cycles, the cycle performance is very sensitive to the adiabatic efficiencies of the rotating equipment and the performance of the off-the-shelf equipment was not sufficient to achieve good cycle efficiency. In addition, large pressure drops occurred in the system due to the instrumentation used, and the long and arduous flow paths. The scroll compressor and expander were found to perform reasonably well considering that they were not designed for the operating conditions encountered.

1. INTRODUCTION

A liquid flooded Ericsson cooler (LFEC) experimental system was designed, built, and tested based on the Type 1 configuration presented by Hugenroth et al. (2006). It is believed that this is the very first prototype that has ever been built based on the liquid flooded Ericsson cycle. Mostly off-the-shelf parts with very little modification were used. The sizing of components used in the system was based on preliminary modeling results for the LFEC 1 cycle. The experimental system was used for proof of concept testing, improvement of a computer model, and to gain design related experience.

The flooded Ericsson cooler concept is based upon the assumption that a compressor and expander can be designed to operate efficiently and reliably while simultaneously compressing or expanding a liquid-gas mixture. This requirement is at odds with the conventional engineering practice of avoiding, by various means, ingestion of liquid into compressors. The primary concern in positive displacement compressors is the incompressibility of the liquid and the extreme loads that are produced within the compressor when trying to do so. However, positive displacement compressors with fixed volume ratios, such as screw and scroll compressors, can operate effectively with large amounts of liquid flooding.

Scroll compressors were the chosen technology for the compressor and expander in the experimental system. They offer several advantages such as being readily available at low cost and at the approximate displacement volume needed. In addition, a scroll compressor can operate as an expander by simply reversing the fluid flow through the machine.

2. EXPERIMENTAL SYSTEM

An experimental system was constructed using primarily off the shelf components. The system was comprised of the following major components; compressor, expander, hydraulic motor, pump, hot and cold separators, hot

and cold mixers, hot and cold heat exchangers, and a regenerator. Nitrogen and alkyl-benzene oil were used as the refrigerant and flooding liquid in the experimental system. Open drive scroll compressors in a bolted housing were selected for the compressor and expander in the system. The absence of a hermetic motor and the ability to easily get inside the compressor to make modifications were very advantageous. In addition, the compressors used had roller element bearings that are less susceptible to damage during adverse lubrication conditions.

A commercially available hydraulic motor and pump were used in the system. These were also open drive components. The separators used in the system were custom built units. The first stage of this utilized simple gravity separation of the liquid from the gas. Additionally, a second stage of separation was used to separate the remaining oil from the gas streams. The second stage separators were commercially available centrifugal type oil separators. The mixing of the liquid and gas streams was accomplished simply by bringing the two streams together at a tee in the lines.

Commercially available heat exchangers were used in the system. The heat exchangers exchanged heat with an aqueous ethylene glycol coolant supplied by a chiller system. The regenerator was also a commercially available heat exchanger.

The compressor, expander, hydraulic motor, and pump were coupled to electric motors. This allowed for independent control of the speed of each component. The expander and hydraulic motor produced power and the electric motors coupled to these components operated regeneratively. Torque cells were placed between the motor shafts and the shaft of each piece of rotating machinery. Torque measurements were used for calculating the power produced or consumed from each component.

Pressure transducers and thermocouples were located between each component in the system. The flow in the liquid loops and gas loop were also measured. In addition, the temperatures and flow rates of coolant flows were also measured. The data were collected by an HP75000 data acquisition system that was connected to a PC. A schematic of the system is shown in Figure 1.

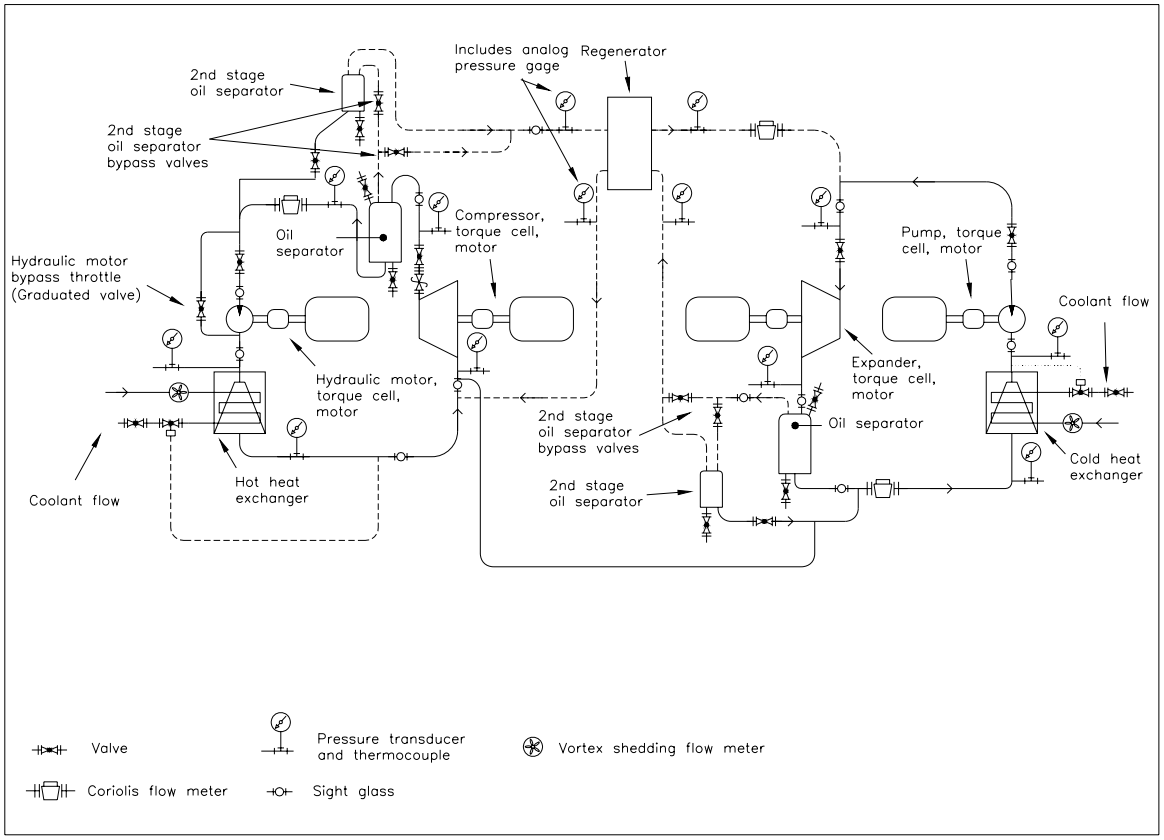

Figure 1: Schematic of the LFEC experimental system.

3. EXPERIMENTAL RESULTS

Approximately 70 tests were run with the experimental system at a number of conditions. Volumetric capacities of over 110 kJ/m^3 were measured. The best second law efficiency was a little over 3%. The poor performance for the experimental system was anticipated. One contributing factor was the large physical size of the system compared to the system's cooling capacity. This led to significant heat gains on the cold side of the system that resulted in a loss in capacity. The large amount of instrumentation contributed to excessive pressure drops in the system. Additionally, excessive pressure drops in the long line sets, with many awkward bends, and sharp angles contributed to the poor performance. The compressor and expander were also major contributors to the overall poor performance of the experimental system. However, the shortcomings of the experimental system that resulted in poor performance were to be expected in early stage development work, such as that presented here.

The experimental program revealed several design related shortcomings of the load stand. Some of these were due to the fact that the system was designed when the computer modeling of the cycle was still in an early stage of development. In addition, the necessity of using off the shelf hardware for most of the major system components led to further limitations of the load stand. The significant operating limitations of the system were as follows:

- The desired heat exchanger set point temperatures could not be reliably specified.
- The low side pressure on the pump was limited to 689 kPa to prevent shaft seal damage.
- Incomplete separation of the oil and gas caused flow measurement errors.
- The system was physically large compared to the cooling capacity produced resulting in significant heat losses and gains at locations other than the heat exchangers.

- It was not generally possible to vary one input parameter between tests while holding the remaining parameters constant.

Despite the limitations of the experimental system, it proved to be an invaluable research tool.

Due to space limitations, a limited amount of the experimental results are presented. The results presented are limited to selected analyses of the compressor and the complete system. Some comments are made with respect to the remaining components in the system. It was stated that limitations in the experimental system made it difficult to vary just one parameter between tests runs. Therefore, in order to analyze performance trends it was necessary to develop regression models based on the experimental data.

3.1 Compressor Experimental Results

The performance trends for the scroll compressor operating under liquid flooded conditions are discussed in the analysis that follows. The curves shown in the figures are from regression models that were developed from the experimental data.

In Figure 2, the adiabatic efficiency of the compressor is plotted as a function of pressure ratio for C_{ratio} values of 5 and 10, where C_{ratio} is defined as the capacitance rate of the oil (i.e. mass flow rate times specific heat) divided by the capacitance rate of the gas. The efficiency decreases with increasing pressure ratio, which is typical for scroll compressors. In the present case, the cause was under-compression loss. The term under-compression refers to when the fluid entrapped in the discharge pockets is at a lower pressure than the high side system pressure. Under-compression loss increases with increasing pressure ratio.

Under-compression loss can be understood with reference to the *PV* diagram shown in Figure 3. The solid line in Figure 3 represents ideal flooded compression for a control mass where the volume shown is that of the gas only. The compressor used in the experimental system had a built in volume ratio of 1.8. The dashed and dotted lines in the figure illustrate what occurs at this volume ratio. During the closed compression process, the *PV* curve for ideal and under-compression are identical. When the closed compression process ends at an overall volume ratio of 1.8, the gas in the compression pockets is exposed to the higher pressure fluid in the system. This event, assumed instantaneous here, raises the pressure in the compression pockets to that of the system. Additional *PV* work is then required to push the higher pressure gas out of the discharge pockets. The area between the ideal compression curve and the under-compression curves represents the additional work required to compress the fluid. In the absence of any other irreversibility, under-compression alone will substantially limit the compressor efficiency. For the compressor and conditions considered in this study, the maximum adiabatic compressor efficiency was approximately 84% at a pressure ratio of 3.5, and 70% at a pressure ratio of 5. When the compressor efficiencies determined from measurements are viewed in the context of the maximum attainable efficiencies when under-compression is occurring, the actual compressor performance was quite good.

For most of the pressure range plotted in Figure 2, the efficiency of the compressor was better at the lower oil flow rate (C_{ratio} of 5 instead of 10). The negative dependence on oil flow rate in this range may be due to the effect of oil flow on discharge port pressure drop. Experimental measurements showed that the pressure drop between the discharge port and the discharge line was significant and increased with C_{ratio}. The large pressure drop was mostly likely due to a discharge port in the fixed scroll of the compressor that was not sized to handle relatively large gas and liquid flows for this flooded compressor.

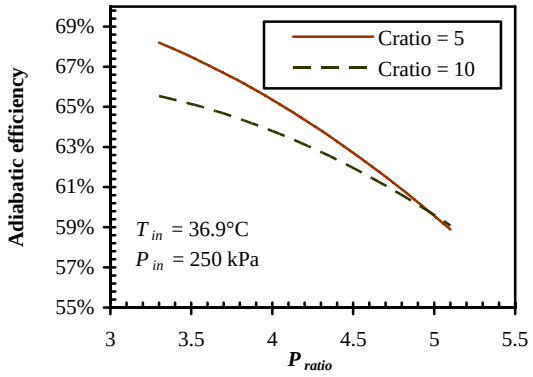

Figure 2: Experimental results for compressor adiabatic efficiency as a function of P_{ratio}.

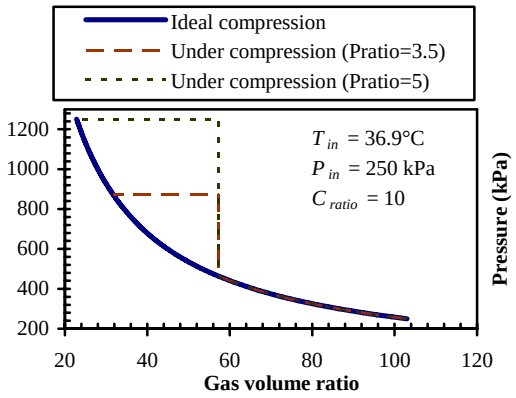

Figure 3: Pressure/volume ratio diagram showing under compression loss.

Figure 4 shows compressor efficiency from a regression model as a function of C_{ratio}, for pressure ratios of 3.5 and 5. The efficiency tends to fall off at higher C_{ratio} values. The effect was more substantial at lower pressure ratios. In addition to the impact of oil flow on pressure drop through the discharge port, it is believed that greater viscous losses within the compressor occurred at high C_{ratio} values. However, this effect was not verified. Additional work is needed to gain a better understanding of this behavior.

Figure 5 shows compressor power as a function of C_{ratio} for pressure ratios of 3.5 and 5, where the power was normalized with respect to the highest power for each case. The power increases as the C_{ratio} value increases. This is due to an increase in liquid pumping power and a decrease in adiabatic efficiency. The results are in general agreement with model predictions (Hugenroth et al., 2006) when variations in the adiabatic and volumetric efficiency are considered.

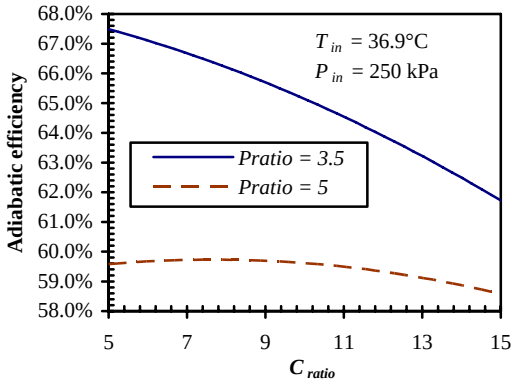

Figure 4: Compressor efficiency as a function of C_{ratio}.

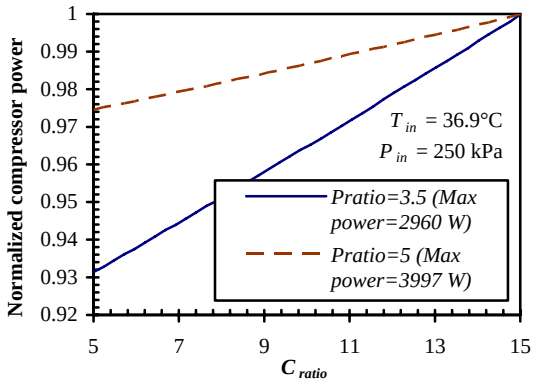

Figure 5: Pressure/volume ratio diagram showing under compression loss.

Figure 6 shows discharge temperature for the compressor as a function of pressure ratio for three C_{ratio} values. Temperature was nondimensionalized with respect to compressor inlet temperature. Figure 7 shows nondimensional compressor discharge temperature as a function of C_{ratio} for pressure ratios of 3.5 and 5. As expected, discharge temperature increased with pressure ratio and decreased with C_{ratio}. For dry compression of nitrogen at the inlet conditions shown in Figures 6 and 7, the nondimensional discharge temperature is 1.43 and 1.58 for pressure ratios of 3.5 and 5, respectively.

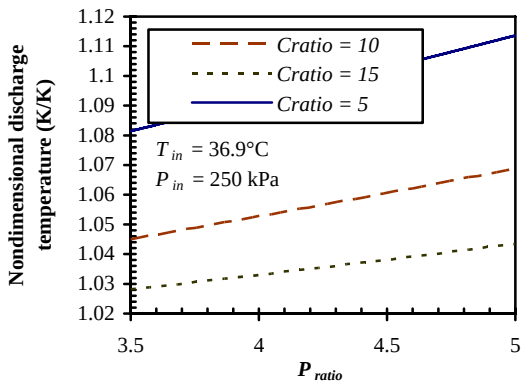

Figure 6: Nondimensional compressor discharge temperature as a function of P_{ratio} for three C_{ratio} values.

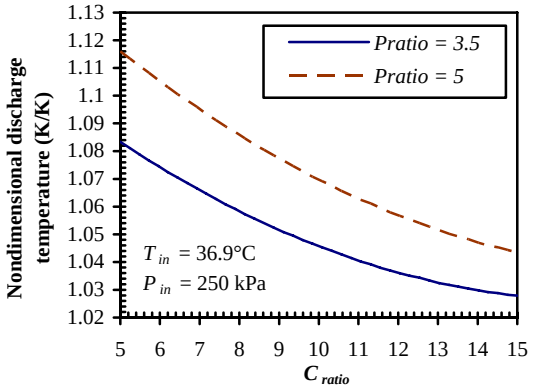

Figure 7: Curve fits of nondimensional compressor discharge temperature as a function of C_{ratio} for two P_{ratio} values.

The volumetric efficiency of the compressor ranged from about 89% to 97% and tended to decrease with increasing pressure differential. This behavior is indicative of internal leakage, which is surprising considering the amount of oil flooding that was occurring. However, modifications were made to the compressor that impacted the flank sealing and could have contributed to this behavior.

A teardown inspection was performed on the compressor after the testing was completed. The scrolls appeared to be in excellent condition. No detrimental impact from the liquid flooding was apparent. The total run time on the compressor was over 200 hours.

3.2 Experimental Results for the Remaining Components in the System

Space requirements preclude a detailed discussion of the experimental results for the remaining components in the system. However, some general observations can be noted. The adiabatic efficiency for the expander ranged from about 51% to 66%. The volumetric efficiency for the expander was not as good as that of the compressor. This was attributed to, and found to correlate with, the much lower running speeds for the expander. The expander shaft speed was the primary means of controlling the pressure ratio of the system. The shaft speed ranged from ¼ to ½ that of the compressor, which was 3500 RPM. At lower speeds, leakage flows across seals between scroll chambers are a larger percentage of the total flow rate than at higher speeds.

The performance of the regenerator in the experimental system was satisfactory with an average effectiveness value of about 82%. The hot and cold heat exchangers performed satisfactorily with the exception that the hot heat exchanger was undersized. The separators used in the system were not able to remove all of the gas from the oil flows. This resulted in gas being entrained within the oil flow in the liquid loops. The presence of gas in the liquid loops had an impact on the performance of the hydraulic motor and pump. In addition, it caused flow measurement errors in the Coriolis-effect mass flow meters.

3.3 Experimental Results for the Complete Cycle

Figures 8 through 11 show selected experimental results for the complete cycle. Figures 8 and 9 show the energy balance error for the experimental system for the 42 test runs that were used in the experimental analysis. The errors are plotted as a function of the hot heat exchanger oil outlet temperature. In Figure 8, the energy balance error is plotted on a volumetric basis, which is the absolute error divided by the compressor displacement rate. In Figure 9, the energy balance error is plotted in relative terms where the relative error is defined as the actual error divided by the sum of the absolute values of the rotating machinery powers and the hot and cold heat exchanger heat transfer rates. That is,

$$Error_{relative} = \frac{\dot{W}_c + \dot{W}_e + \dot{W}_m + \dot{W}_p + \dot{Q}_c + \dot{Q}_h}{\left|\dot{W}_c\right| + \left|\dot{W}_e\right| + \left|\dot{W}_m\right| + \left|\dot{W}_p\right| + \left|\dot{Q}_c\right| + \left|\dot{Q}_h\right|} \quad (1)$$

Both positive errors, where more energy entered the system than left and negative errors were recorded. The correlation between the energy balance error and the hot heat exchanger outlet temperature is readily apparent,

and it reveals the nature of the error. That is, the error was due primarily to heat losses and gains throughout the system. At high heat exchanger outlet temperatures, the temperature differential between the hot side of the system and the ambient was larger so more heat was lost from the system at locations other than the hot heat exchanger. As the hot heat exchanger outlet temperature approached the ambient temperature, the heat gain to the cold side of the system began to dominate, and the energy balance became negative. The hot heat exchanger temperature varied over a much larger range than the cold heat exchanger temperature. The significant amount of heat leakage that occurred throughout the system was a consequence of the fact that the system was physically large when compared to the capacities that were attained. In addition, the instrumentation on the system was not sufficient to directly measure the heat leakage at various locations in the system.

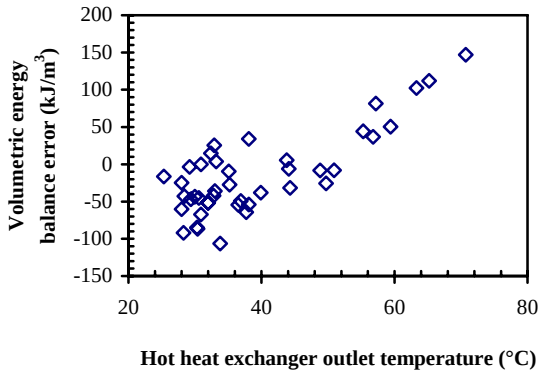

Figure 8: Cycle cooling capacity as a function of compressor pressure ratio for C_{ratio}=11.

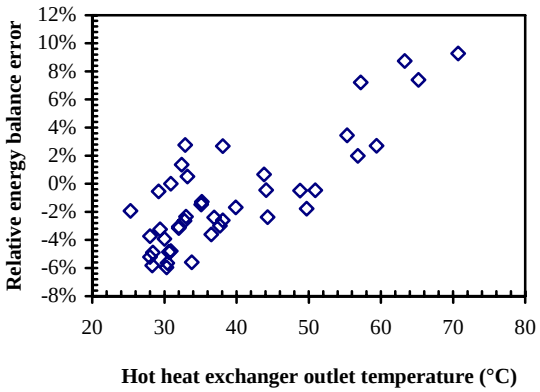

Figure 9: Cycle second law efficiency as a function of compressor pressure ratio for C_{ratio}=11.

The second law efficiency and volumetric capacity are presented in Figures 10 and 11, respectively. The second law efficiency is defined as the measured coefficient of performance (COP) divided by the Carnot COP. The volumetric capacity is defined as the absolute cooling capacity divided by the compressor displacement rate. Volumetric capacity provides a measure that is independent of the physical size of the equipment used in the system. Regression models have been used to permit the display of performance trends. The input parameters used in the plots are shown in Table 1.

Table 1: Input parameters for plots in Figures 8 through 11.

Cold HX oil outlet temperature (°C)	Hot HX oil outlet temperature (°C)	$C_{ratio,c,e}$
2	35	11

In Figure 10, the volumetric capacity is plotted as a function of compressor pressure ratio for three compressor inlet pressures. The volumetric capacity tends to increase with increasing compressor inlet pressure, which is the expected trend. The curves show a capacity maximum at a certain pressure ratio. A monotonic increase is generally expected with increasing pressure ratio. This assumes that component efficiencies are constant and that there are no heat leaks. This was not the case with the experimental system.

In Figure 11, the second law efficiency for the experimental system is shown as a function of compressor pressure ratio for three inlet pressures. The efficiency of the system increases as the compressor inlet pressure decreases, which is consistent with model predictions. It can also be seen that an optimum efficiency value occurs at a particular pressure ratio and the optimum pressure ratio increases with decreasing compressor inlet pressure. Both of these trends are qualitatively consistent with modeling results. However, nonideal behavior that was not modeled, such as pressure drops and variation in component efficiencies, has an impact on the trends shown.

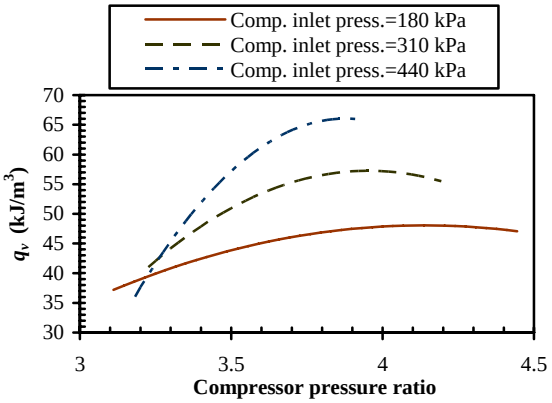

Figure 10: Cycle cooling capacity as a function of compressor pressure ratio for C_{ratio}=11.

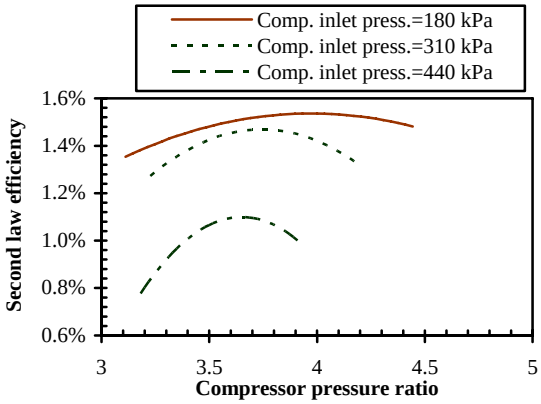

Figure 11: Cycle second law efficiency as a function of compressor pressure ratio for C_{ratio}=11.

4. SUMMARY

An experimental LFEC 1 (Hugenroth et al., 2006) load stand was constructed. Volumetric capacities of up to 110 kJ/m^3 were measured. The efficiency of the load stand was very poor with a maximum recorded second law efficiency of 3%. The poor performance of the load stand was anticipated due in part to the use of off-the-shelf components. In addition, large pressure drops, due to abundant instrumentation, and arduous flow paths, hurt the performance. The load stand was found to have some operating limitations. However, its performance was adequate to meet the needs of the experimental program.

Other than the basic proof of concept goal, another goal of the experimental program was to show that scroll compressors could tolerate the necessary amount of liquid flooding required for the cycle to operate as envisioned. In addition, it was hoped that some estimate could be made as to whether or not a properly designed scroll compressor could reach the adiabatic efficiency that would be required for a commercial system. It was found that the compressor and expander could operate reliably under the flooding conditions. In addition, the adiabatic efficiency of both the compressor and expander were very satisfactory given that they were not designed for the LFEC application.

NOMENCLATURE

C_{ratio}	Capacitance rate ratio	**Subscripts**	
$\dot{Q}$	Heat transfer rate	*c*	Compressor, cold
$\dot{W}$	Power	*e*	Expander
		h	Hot
		m	hydraulic motor
		p	Pump

REFERENCES

Hugenroth, J., Braun, J., Groll, E., King, G., 2006, "Liquid-Flooded Ericsson Cycle Cooler: Part 1- Thermodynamic Analysis", *Proceedings of the 2006 International Refrigeration and Air Conditioning Conference at Purdue*, R168.